

# RSC Advances



This is an *Accepted Manuscript*, which has been through the Royal Society of Chemistry peer review process and has been accepted for publication.

*Accepted Manuscripts* are published online shortly after acceptance, before technical editing, formatting and proof reading. Using this free service, authors can make their results available to the community, in citable form, before we publish the edited article. This *Accepted Manuscript* will be replaced by the edited, formatted and paginated article as soon as this is available.

You can find more information about *Accepted Manuscripts* in the [Information for Authors](#).

Please note that technical editing may introduce minor changes to the text and/or graphics, which may alter content. The journal's standard [Terms & Conditions](#) and the [Ethical guidelines](#) still apply. In no event shall the Royal Society of Chemistry be held responsible for any errors or omissions in this *Accepted Manuscript* or any consequences arising from the use of any information it contains.

**Generation of Cu nanoparticles on novel designed  
Fe<sub>3</sub>O<sub>4</sub>@SiO<sub>2</sub>/EP.EN.EG as reusable nanocatalyst for the reduction  
of nitro compounds**

Maryam Rajabzadeh<sup>a</sup>, Hossein Eshghi<sup>a\*</sup>, Reza Khalifeh<sup>b</sup>, Mehdi Bakavoli<sup>a</sup>

**Abstract**

In this work, Copper nanoparticles loaded on Fe<sub>3</sub>O<sub>4</sub>@SiO<sub>2</sub> which shortly named as Fe<sub>3</sub>O<sub>4</sub>@SiO<sub>2</sub>/EP.EN.EG@Cu has been designed, prepared and characterized by XRD, FTIR, TEM, SEM, EDS, TGA, ICP, successfully. The catalytic performance was investigated in the reduction of aromatic nitro compounds in the presence of NaBH<sub>4</sub> aqueous solution as the source of hydrogen at 50 °C. Fe<sub>3</sub>O<sub>4</sub>@SiO<sub>2</sub>/EP.EN.EG@Cu catalyst was readily removed from the reaction mixture by applying an external magnetic and reused for five times without significant loss of the catalytic activity.

**Keywords:**

Nanocatalyst, Fe<sub>3</sub>O<sub>4</sub>@SiO<sub>2</sub>/EP.EN.EG, Reduction, Aromatic amines

**Introduction:**

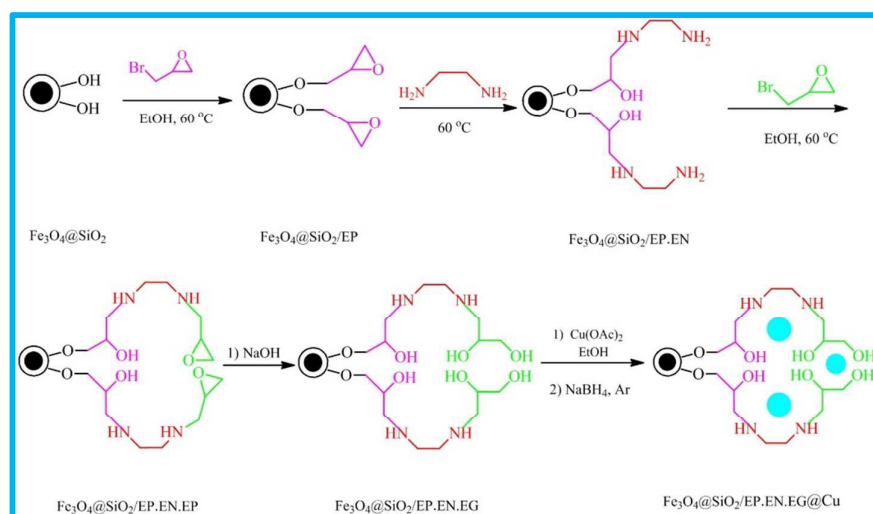
In the past decades, controlled assembly of nanomaterials attracted much attention. Well known copper based catalysts in organic reactions have been given much attention by material scientists and chemists.<sup>1-3</sup> Homogeneous copper based catalysts have been used in many organic transformations, but the many problems are associated with the separation and reusability of catalyst after the reaction that prevent their industrial applications. Therefore, the heterogenization of homogeneous catalyst to provide supported catalysts with high active sites and high surface area became an important protocol. Therefore, design and utilization of a heterogeneous nanocatalyst which can be practically separated easily is desirable.<sup>4-7</sup> Nanocatalysis has shown improved catalytic

activity compared to bulk catalysts. This is due to an increased number of active sites for the smaller versions of the catalysts and high surface to volume ratio as compared to their larger counterparts.<sup>8-11</sup> In family of nanocatalysis, the magnetic nanoparticles have attracted increasing attention because they possess interesting properties which could see potential use in catalysis including nanomaterial-based catalysts,<sup>12</sup> magnetic resonance imaging,<sup>13</sup> drug delivery systems,<sup>14</sup> hyperthermia treatment of cancer cells.<sup>15</sup> In addition, magnetic nanoparticles are easily separated from the reaction mixture by an external magnet and this is described as the more sufficient strategy than conventional techniques such as filtration or centrifugation.<sup>16,17</sup> Unfortunately, naked magnetic nanoparticles are often unstable, readily aggregated and usually don't constitute strong covalent bonds with functionalization molecules. Encapsulation of magnetic nanoparticles in inert matrices such as silica (SiO<sub>2</sub>) can overcome these drawbacks.<sup>18</sup> Magnetic nanoparticles have been extensively applied in various organic reaction, such as C–C bonding formation,<sup>19</sup> dihydroxylation of olefins,<sup>20</sup> oxidation reactions<sup>21</sup> and hydrogenation reaction.<sup>22</sup> Hydrogenation of nitroarene is one of the most useful methods to production of aromatic amines. The amine group are often significant intermediates in the fabrication of many pharmaceuticals, agrochemicals, dyes, polymers, photographic and rubber materials.<sup>23</sup> There are common methods to reduce a nitro precursor: metal/acid reduction,<sup>24-26</sup> catalytic hydrogenation,<sup>27</sup> homogeneous catalytic transfer hydrogenation<sup>28</sup> and heterogeneous catalytic transfer hydrogenation.<sup>29,30</sup> However, these approaches have several major drawbacks: metal/acid system has shown poor selectivity and this methodology is environmentally dangerous, catalytic hydrogenation is undesirable due to use of H<sub>2</sub> gas at high pressure and temperature, the separation of homogeneous or heterogeneous catalytic transfer hydrogenation, from the final product is difficult.<sup>31,32</sup> Therefore, it is necessary to find new catalysts for hydrogenation of nitro arenes under

mild conditions. In this paper we wish, to report preparation of functionalized magnetic nanoparticles  $\text{Fe}_3\text{O}_4@\text{SiO}_2/\text{EP}.\text{EN}.\text{EG}$  and *in situ* generation of Cu NPs as excellent catalytic efficiency and the catalytic activity has been estimate by the reduction of nitroarens to amin with  $\text{NaBH}_4$  under mild aqueous condition.

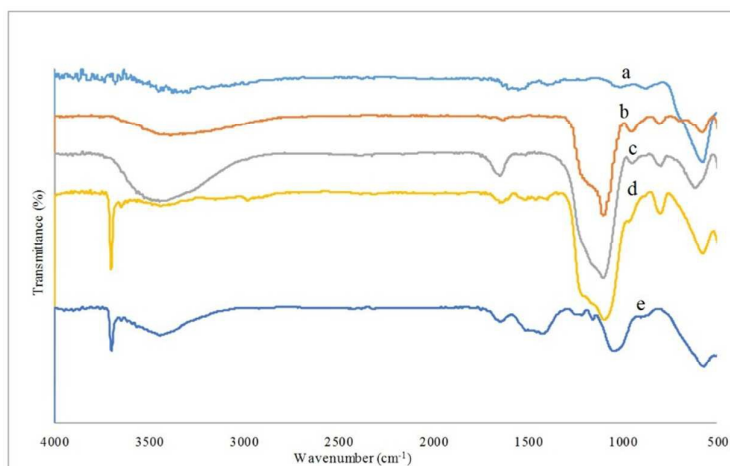
## Results and discussion

As shown in Scheme 1, the  $\text{Fe}_3\text{O}_4@\text{SiO}_2/\text{EP}.\text{EN}.\text{EG}@\text{Cu}$  nanocatalyst was prepared in 4 steps: in first step the  $\text{Fe}_3\text{O}_4@\text{SiO}_2$  magnetic nanoparticles was synthesized by Stöber sol-gel method,<sup>33</sup> in step 2, EP.EN.EG linker as novel designed ligand covalently bonded on surface hydroxyl groups of silica coated magnetic nanoparticles. In step 3, the ligands was activated with NaOH and then  $\text{Cu}(\text{OAc})_2$  was complexed to this N, N, O type ligand. Finally in step 4, Cu nanoparticles was generated with  $\text{NaBH}_4$  reduction procedure. The synthesized  $\text{Fe}_3\text{O}_4@\text{SiO}_2/\text{EP}.\text{EN}.\text{EG}@\text{Cu}$  was characterized by FT-IR, thermo gravimetric analysis (TGA), scanning electron microscopy (SEM), transmission electron microscopy (TEM), energy dispersive X-ray (EDS), X-ray diffraction (XRD) and vibrating sample magnetometer (VSM).



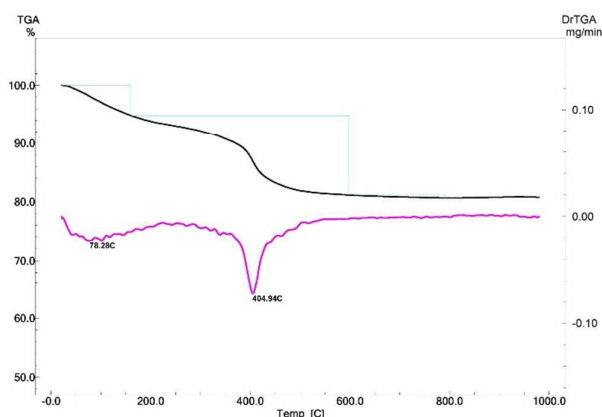
**Scheme 1** Preparation process of the  $\text{Fe}_3\text{O}_4@\text{SiO}_2/\text{EP}.\text{EN}.\text{EG}@\text{Cu}$

FTIR was used to characterize the surface constructure of the synthesized materials, as shown in Figure 1. The strong absorption bands at  $573\text{ cm}^{-1}$  can be attributed to the stretching vibration of the Fe–O bond, which confirms the existence of  $\text{Fe}_3\text{O}_4$ . The broad characteristic band  $3444\text{ cm}^{-1}$  is related to stretching vibration O–H, demonstrating the presence of hydroxyl groups on the surface of  $\text{Fe}_3\text{O}_4$  MNPs (Figure 1a). Comparison with Figure 1a, 1b shows, that the intensity of Fe–O bond significantly weakens and a strong absorption peak at  $1098\text{ cm}^{-1}$  and weak absorption peak at  $953\text{ cm}^{-1}$  was appeared. This can be assigned to asymmetric vibration of the Si–O–Si bond and the symmetric stretching of the Si–OH bond, respectively, which suggests that  $\text{Fe}_3\text{O}_4$  was effectively coated with a silica layer. The epoxy rings which are anchored on the surface of silica coated magnetic nanoparticles are characterized by the methylene C–H stretching<sup>34</sup> at  $3050\text{ cm}^{-1}$  and C–O–C vibration stretching<sup>35</sup> at  $1260\text{--}1240\text{ cm}^{-1}$ . In both cases, vibration frequency was covered by the broad band of stretching vibration O–H and asymmetric vibration of the Si–O–Si bond, respectively. The absorption band of stretching vibration O–H and asymmetric vibration of the Si–O–Si bond are getting more broadened which is clearly observed in the Figure 1c in comparison to 1b. As shown in Figure 1d broad absorption band in the  $3436\text{ cm}^{-1}$  are ascribed to the stretching vibration of O–H and  $\text{--NH}_2$  and the band at  $3700\text{ cm}^{-1}$  are due to stretching of the N–H bonds or an overtone peaks of C–O stretching bands at  $1233\text{ cm}^{-1}$ . Increasing of the intensity of the O–H and N–H stretching vibration can suggest the attachment of the second epoxy ring to catalyst (as shown in Figure 1e).



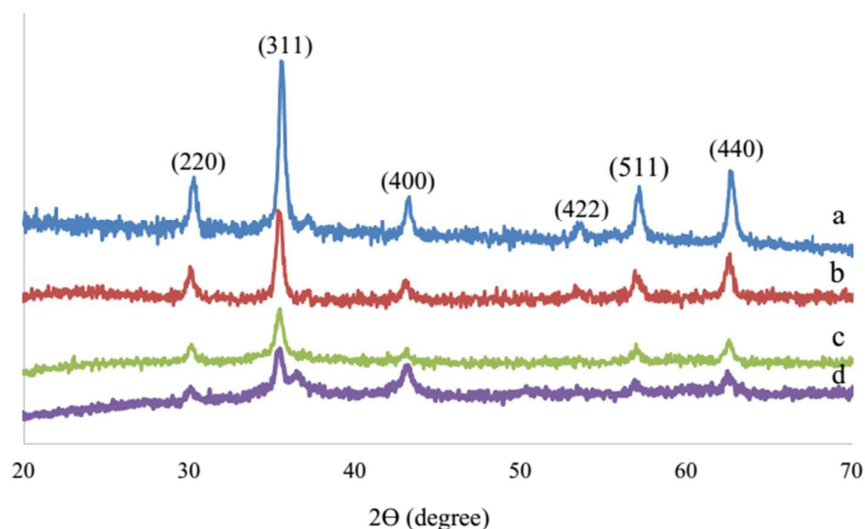
**Figure 1** FTIR spectrum of  $\text{Fe}_3\text{O}_4$ (a),  $\text{Fe}_3\text{O}_4@\text{SiO}_2$  (b),  $\text{Fe}_3\text{O}_4@\text{SiO}_2.\text{EP}$  (c),  $\text{Fe}_3\text{O}_4@\text{SiO}_2.\text{EP}.\text{EN}$ (d),  $\text{Fe}_3\text{O}_4@\text{SiO}_2.\text{EP}.\text{EN}.\text{EG}$  (e)

The thermal stability of the  $\text{Fe}_3\text{O}_4@\text{SiO}_2/\text{EP}.\text{EN}.\text{EG}$  was characterized by thermogravimetric analysis (TGA). TGA curves in Figure 2 demonstrate the weight loss around  $100^\circ\text{C}$  which was related to the loss of absorbed water molecules on the support. The weight loss of 13% in the temperature range of  $190\text{--}600^\circ\text{C}$  which was attributed to the decomposition of organic parts that were grafted on the surface of  $\text{Fe}_3\text{O}_4@\text{SiO}_2$  and amount of anchored content was evaluated to be  $0.6\text{ mmol g}^{-1}$ . Therefore, the result confirms that the ligand grafting had been successfully achieved.



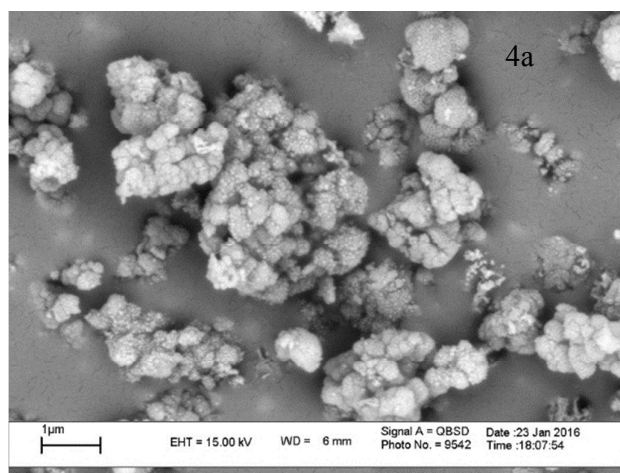
**Figure 2** TG analysis of  $\text{Fe}_3\text{O}_4@\text{SiO}_2/\text{EP}.\text{EN}.\text{EG}$

The crystal structure of  $\text{Fe}_3\text{O}_4$ ,  $\text{Fe}_3\text{O}_4@\text{SiO}_2$  and  $\text{Fe}_3\text{O}_4@\text{SiO}_2/\text{EP.EN.EG}@\text{Cu}$  were characterized by XRD. As shown in Figure 3, six characteristic peaks at  $2\theta = 30.31$ ,  $35.64$ ,  $43.31$ ,  $53.86$ ,  $57.24$ ,  $62.83$ , which attributed to the (220), (311), (400), (422), (511), (440) crystal planes confirm well with the standard  $\text{Fe}_3\text{O}_4$  (cubic phase). Figure 3b Shows a new broad peak at  $2\theta = 23$  which can be attributed to the amorphous silica shell. Compared with curve b, we find that no remarkable change occurs in the number of peaks in curve c, only a slight decline in the intensity of the diffraction peaks indicating retained crystal structure of the  $\text{Fe}_3\text{O}_4$  core after immobilization of Cu nanoparticles. No peaks of Cu nanoparticles was observed in the XRD pattern due to the disperse of Cu nanoparticles in the catalysis matrix. So, Cu nanoparticles cannot lead to the formation of regular crystal lattice. The presence of Cu nanoparticles was verified through the analysis of ICP and EDS technigues.



**Figure 3** XRD pattern of  $\text{Fe}_3\text{O}_4$  (a),  $\text{Fe}_3\text{O}_4@\text{SiO}_2$  (b) and  $\text{Fe}_3\text{O}_4@\text{SiO}_2/\text{EP.EN.EG}@\text{Cu}$  (c).  $\text{Fe}_3\text{O}_4@\text{SiO}_2/\text{EP.EN.EG}@\text{Cu}$  catalyst after five recoveries (d).

Figure 4a shows the SEM image of  $\text{Fe}_3\text{O}_4@\text{SiO}_2/\text{EP.EN.EG}@\text{Cu}$  nanocatalyst. Based on 4a spherical morphology of nanocatalyst is clearly observed. Moreover, to further investigate the morphologies and particle size of  $\text{Fe}_3\text{O}_4@\text{SiO}_2$ , and  $\text{Fe}_3\text{O}_4@\text{SiO}_2/\text{EP.EN.EG}@\text{Cu}$ , TEM images of catalyst were studied. TEM images of 4b indicate the spherical structure of  $\text{Fe}_3\text{O}_4@\text{SiO}_2$  and each nanocomposite contains several  $\text{Fe}_3\text{O}_4$  nano particles in one  $\text{SiO}_2$  shell, which results in the nano composites demonstrating strong magnetic properties.<sup>32</sup> also the average size of MNPs is about 20 nm. As expected, the as prepared  $\text{Fe}_3\text{O}_4@\text{SiO}_2/\text{EP.EN.EG}@\text{Cu}$  has the spherical shape (Figure 4c), which indicates, spherical structure has not significantly influenced after immobilization of Cu nanoparticle on the surface of  $\text{Fe}_3\text{O}_4@\text{SiO}_2$  support. In addition, the attendance of Fe, Si and Cu elements are shown in EDS spectrum (Figure 4d). It also confirmed our design to the existence of  $\text{Fe}_3\text{O}_4$ ,  $\text{SiO}_2$  and Cu nanoelements in this catalyst. The copper amounts of catalyst were determined by inductively coupled plasma (ICP)  $2.29 \text{ mmol g}^{-1}$ .





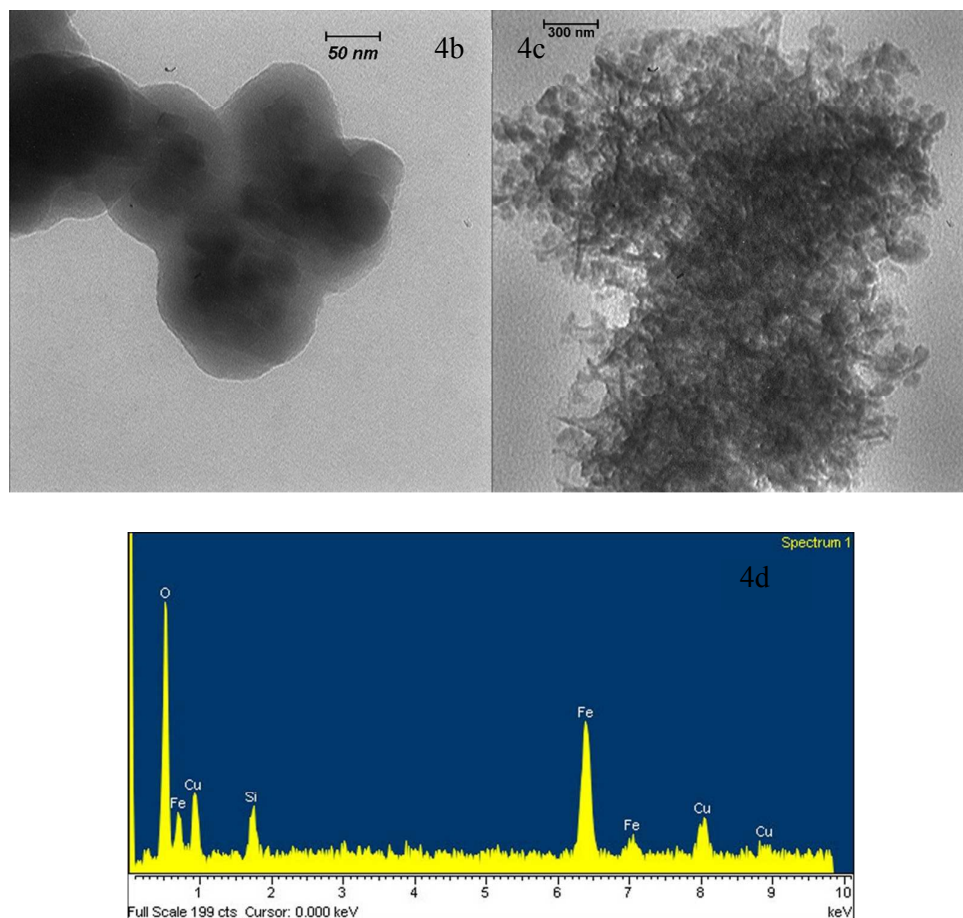


**Figure 4** SEM images of Fe<sub>3</sub>O<sub>4</sub>@SiO<sub>2</sub>/EP.EN.EG@Cu (a). TEM images of the Fe<sub>3</sub>O<sub>4</sub>@SiO<sub>2</sub> (b). Fe<sub>3</sub>O<sub>4</sub>@SiO<sub>2</sub>/EP.EN.EG@Cu (c). EDS spectrum of the Fe<sub>3</sub>O<sub>4</sub>@SiO<sub>2</sub>/EP.EN.EG@Cu (d).

For magnetic designed materials, the magnetic responsivity is very important. Therefore, the magnetic properties of the Fe<sub>3</sub>O<sub>4</sub>, Fe<sub>3</sub>O<sub>4</sub>@SiO<sub>2</sub> and Fe<sub>3</sub>O<sub>4</sub>@SiO<sub>2</sub>/EP.EN.EG@Cu were analyzed by VSM (vibrating sample magnetometer) at room temperature, as shown in Figure 5. As can be seen, the saturation magnetization (Ms) value of the above magnetic samples are 63.6, 37.8 and 29.4, respectively. These results indicated the decrease in Ms values for Fe<sub>3</sub>O<sub>4</sub>@SiO<sub>2</sub> and Fe<sub>3</sub>O<sub>4</sub>@SiO<sub>2</sub>/EP.EN.EG@Cu in comparison to uncoated Fe<sub>3</sub>O<sub>4</sub>. These decreases are due

to increase in mass and size after coating the SiO<sub>2</sub> shell and anchoring the Cu nanoparticles. Also, in the magnetization curves no noticeable remanence or coercivity was observed, which confirms superpara magnetic character. So, the new magnetic materials can be easily separated by an external magnet.

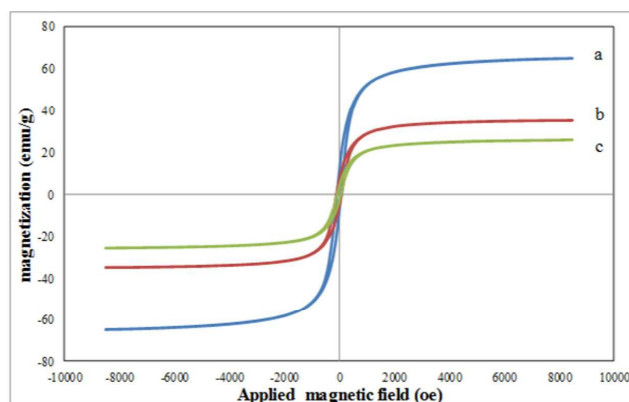
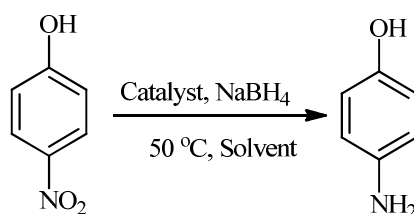


**Figure 5** Magnetization curve of Fe<sub>3</sub>O<sub>4</sub> (a), Fe<sub>3</sub>O<sub>4</sub>@SiO<sub>2</sub> (b), Fe<sub>3</sub>O<sub>4</sub>@SiO<sub>2</sub>/EP.EN. EG@Cu (c).

The catalytic performance of the novel Fe<sub>3</sub>O<sub>4</sub>@SiO<sub>2</sub>/EP.EN. EG@Cu as a magnetically nanocatalyst was investigated for the reduction of aromatic nitro compounds. The reduction reaction of para-nitrophenol in the presence of NaBH<sub>4</sub> as the source of hydrogen (Equation I) was chosen as a model reaction to optimize the reaction conditions. At first, the effect of solvent and molar ratio of hydrogen sources on the model reaction were examined. (Table 1, entries 1-10) It was found that water was the best solvent for the model reaction when 3.0 mmol NaBH<sub>4</sub> as hydrogen source were used and the product was obtained in 98% yield. (Table 1, entry 5) A rise in the amount of NaBH<sub>4</sub> from 0.1 mmol to 3.0 mmol caused increment in the rate of reduction of para-nitrophenol (Table 1, entries 1-5). Reduction was very slow in aprotic solvents such as THF, DMF (Table 1, entries 7-8) and non-polar solvent like toluene (Table 1, entry 10). The employment of a protic solvents for example EtOH, CH<sub>3</sub>OH, H<sub>2</sub>O was the most

suitable for this catalytic system (Table 1, entries 5-7), H<sub>2</sub>O was selected for the nitroarene reduction because it is generally considered as inexpensive, safe, and environmentally green solvent.

**Table 1** Reduction of para -nitrophenol in the presence of different amounts of NaBH<sub>4</sub> in various solvents by Fe<sub>3</sub>O<sub>4</sub>@SiO<sub>2</sub>/EP.EN.EG@Cu



(Equation I)

Entry	Hydrogen source	Solvent	Time(min)	Yield[%]
1	NaBH <sub>4</sub> (0.1mmol)	H <sub>2</sub> O	60	40
2	NaBH <sub>4</sub> (0.5mmol)	H <sub>2</sub> O	60	40
3	NaBH <sub>4</sub> (1mmol)	H <sub>2</sub> O	45	60
4	NaBH <sub>4</sub> (2mmol)	H <sub>2</sub> O	45	90
5	NaBH <sub>4</sub> (3mmol)	H <sub>2</sub> O	15	98
6	NaBH <sub>4</sub> (3mmol)	EtOH	20	95
7	NaBH <sub>4</sub> (3mmol)	CH <sub>3</sub> OH	30	90
8	NaBH <sub>4</sub> (3mmol)	THF	120	20
9	NaBH <sub>4</sub> (3mmol)	DMF	120	40
10	NaBH <sub>4</sub> (3mmol)	Toluene	240	20

The influence of catalyst amount was investigated on the model reaction. No progress in the reduction of aromatic nitro compounds was observed neither in the absence of catalyst nor in the presence of Fe<sub>3</sub>O<sub>4</sub>@SiO<sub>2</sub>/EP.EN.EG. Results in Table 2 shows that, the increasement of the amount of catalyst from 0.001 to 0.05 g per mmol of substrate, (Table 2, entries3-7) results an increased reaction yield and the maximum yield (98%) has been achieved in the presence of 0.05g of catalyst, (Table 2, entry 7). The results are in good agreement with significant rise in the number of active sites.

**Table 2** Yield% dependence on the amount of Fe<sub>3</sub>O<sub>4</sub>@SiO<sub>2</sub>/EP.EN.EG@Cu

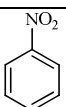
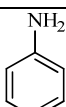
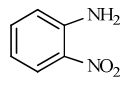
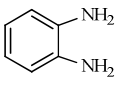
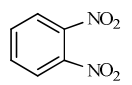
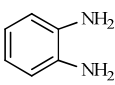
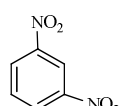
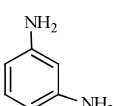
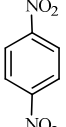
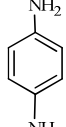
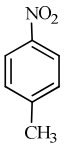
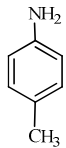
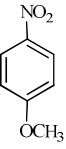
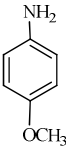
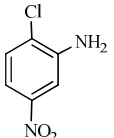
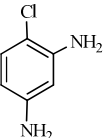
Entry	amount of catalyst (g)	Time (min)	Yield (%)
1 <sup>a</sup>	-	15	0
2	Fe <sub>3</sub> O <sub>4</sub> @SiO <sub>2</sub> /EP.EN.EG	15	0
3	0.001	240	50
4	0.005	120	50
5	0.01	90	70
6	0.03	45	85
7	0.05	15	98

<sup>a</sup>In the presence of NaBH<sub>4</sub>

As shown in Table 3, we employed the optimized conditions for the conversion of nitro aromatic containing different functional group into the corresponding amino compounds (Table 3, entries 1-15). The results of Table 3 indicate, electron with drawing/donating substituents do not have a remarkable influence on the reaction times and yields. Sensitive functional groups, such as -OH, -Cl, -CH<sub>3</sub>, -COOH, -CN, -COCH<sub>3</sub>, -OCH<sub>3</sub> and -NHCOCH<sub>3</sub> remained intact during the reduction of nitro group (Table 3, entries 6-14). Dinitro compounds were successfully transformed to the corresponding diamines, which are important precursor for many heterocyclic compounds and used as a component of engineering polymers and composites (Table 3, entries 3-5). Aldehyde carbonyl groups in the nitro compounds were not compatible with the reaction condition and reduction happens for both functional groups. (Table 3, entry 15). According to steric effect that has been observed, the existence of electron with drawing/donating groups, ortho or meta to the nitro group increased the reaction time than at the para position. Therefore, these investigation indicated Fe<sub>3</sub>O<sub>4</sub>@SiO<sub>2</sub>/EP.EN.EG@Cu catalyst

system was also effective for the reduction of nitro aryl compounds with high yields and short reaction times in water.

**Table 3** Reduction of various nitro aromatic compounds over  $\text{Fe}_3\text{O}_4@\text{SiO}_2/\text{EP.EN.EG}@\text{Cu}$  catalyst

Entry	Reactant	Product	Time(min)	Yield(%) <sup>a</sup>	Mp(°C)
1			15	85	-
2			8	98	100-102 °C (Lit. 101-104 °C) <sup>37</sup>
3			10	98	100-102 °C (Lit. 101-104 °C) <sup>37</sup>
4			8	95	64-66 °C (Lit. 63-65 °C) <sup>37</sup>
5			5	100	139-140 °C (Lit. 139-141 °C) <sup>37</sup>
6			10	95	40-41 °C (Lit. 40-41 °C) <sup>38</sup>
7			10	95	57-59 °C (Lit. 57 °C) <sup>39</sup>
8			5	98	62-64 °C (Lit. 62-66 °C) <sup>40</sup>

9			Immediately	100	203-205 (Lit. 203-204 °C) <sup>41</sup>
10			15	98	185-187 °C (Lit. 187-189 °C) <sup>42</sup>
11			20	90	202-204 °C (lit. 204-205 °C) <sup>43</sup>
12			15	95	104-106 °C (Lit. 102-104 °C) <sup>44</sup>
13			5	100	182-185 °C (lit. 185-186 °C) <sup>45</sup>
14			5	95	169-170 °C (Lit. 172-173 °C) <sup>45</sup>
15			Immediately	100	90-92 °C (Lit. 90-92 °C) <sup>38</sup>

a) Isolated yield

The reduction of p-nitrophenol to p-aminophenol using  $\text{NaBH}_4$  as reductant and the  $\text{Fe}_3\text{O}_4@\text{SiO}_2/\text{EP.EN.EG}@\text{Cu}$  as the catalyst was studied by UV-Vis spectroscopy. The presence of both the reactant p-nitrophenolate anion ( $\lambda_{\text{max}} = 400 \text{ nm}$ ) and the product p-AP ( $\lambda_{\text{max}} = 300 \text{ nm}$ ) can be convincingly demonstrated by the UV/Visible absorption spectroscopy (Figure 6a). Linear relationships of  $\ln(C_t/C_0)$  versus reaction time was shown in Figure 6b. Therefore, the reduction of p-Nitrophenol follows the pseudo-first order kinetics. The rate constant  $k$  is calculated to be  $3.2 \times 10^{-3} \text{ s}^{-1}$ .

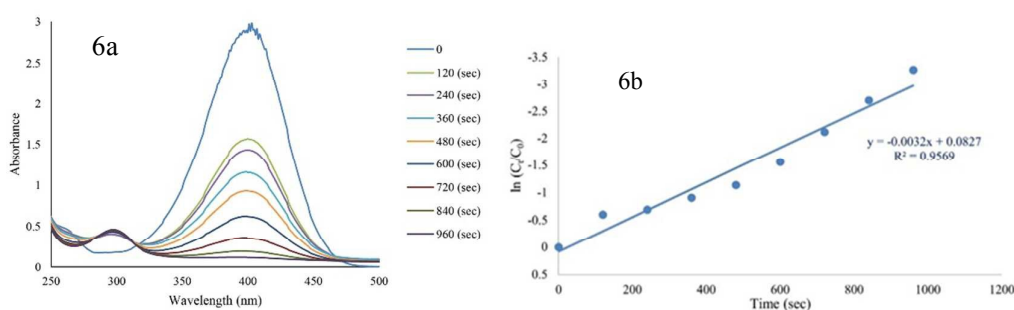


**Figure 6** UV/Visible spectrum of the absorption spectra of mixture of p-nitrophenol and  $\text{NaBH}_4$  in presence of  $\text{Fe}_3\text{O}_4@\text{SiO}_2/\text{EP.EN.EG}@\text{Cu}$  at different time (a), Plots of  $\ln(C_t/C_0)$  versus reaction time (b). Reaction condition: p-nitrophenol ( $5 \times 10^{-3} \text{ M}$ ),  $\text{NaBH}_4$  (0.5mM) and catalyst (0.08 mol%) at  $50^\circ\text{C}$

The reuse ability of a catalyst is very important for a catalytic process. The  $\text{Fe}_3\text{O}_4@\text{SiO}_2/\text{EP.EN.EG}@\text{Cu}$  catalyst was separated by an external magnet, was washed with ethanol to remove the organic impurities, was dried at room temperature and the catalyst was reused for at least 5 times. The result is presented in Table 4 and indicates that the catalytic activity of  $\text{Fe}_3\text{O}_4@\text{SiO}_2/\text{EP.EN.EG}@\text{Cu}$  did not decrease after 5 consecutive cycles.

**Table 4** The catalyst reusability for the reduction of para-nitrophenol

Run	Time(min)	Yield(%)
1	15	98
2	15	98
3	15	98
4	15	95
5	15	95

The kinetic reusability of  $\text{Fe}_3\text{O}_4@\text{SiO}_2/\text{EP.EN.EG}@\text{Cu}$  in the reduction of p-Nitrophenol was studied (Figure 7). Results demonstrate that  $\text{Fe}_3\text{O}_4@\text{SiO}_2/\text{EP.EN.EG}@\text{Cu}$  can be reused for at least 5 times. Based on these results, the reaction was not completed even after 60 min for recycle 6. The catalyst was recovered by an external magnetic field and then was washed with water and ethanol to remove any absorbed products.

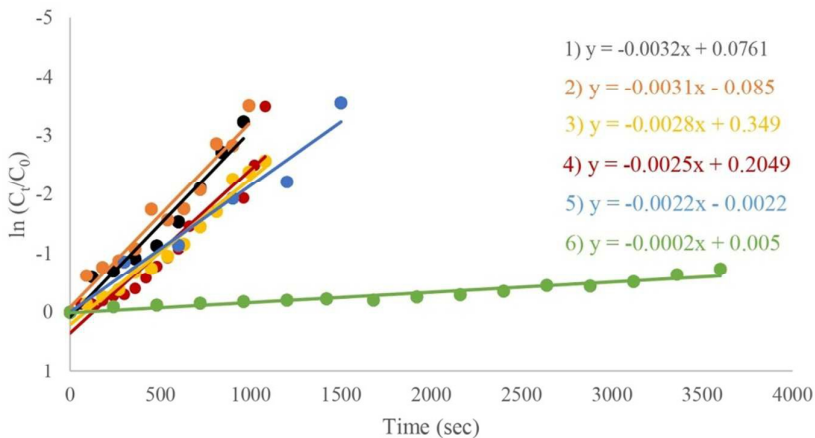


**Figure 7** Plots of  $\ln(C_t/C_0)$  versus reaction time for each of  $\text{Fe}_3\text{O}_4@\text{SiO}_2/\text{EP.EN.EG}@\text{Cu}$  recyclability



Comparison of TEM image, SEM image (Figure 8) of reused catalyst with fresh catalysts (Figure 4a, 4b, 4c) showed that the morphology and structure of  $\text{Fe}_3\text{O}_4@\text{SiO}_2/\text{EP.EN.EG}@\text{Cu}$  catalyst was remained intact after five recoveries. The XRD pattern of reused  $\text{Fe}_3\text{O}_4@\text{SiO}_2/\text{EP.EN.EG}@\text{Cu}$  catalyst is shown in Figure 3d, revealed that the  $\text{Fe}_3\text{O}_4$  retain its magnetite crystalline structure after the 5 runs. In additionally, new characteristic diffraction peaks at  $2\theta = 36.88, 42.48$  of  $\text{Cu}_2\text{O}$  can be observed after 5 times reused of catalyst, which indicated to the reaction between small amount of Cu nanoparticles and the air  $\text{O}_2$  due to successive performing. Furthermore, the copper amounts of catalyst after five times reuse was determined by inductively coupled plasma (ICP)  $1.22 \text{ mmol g}^{-1}$ .

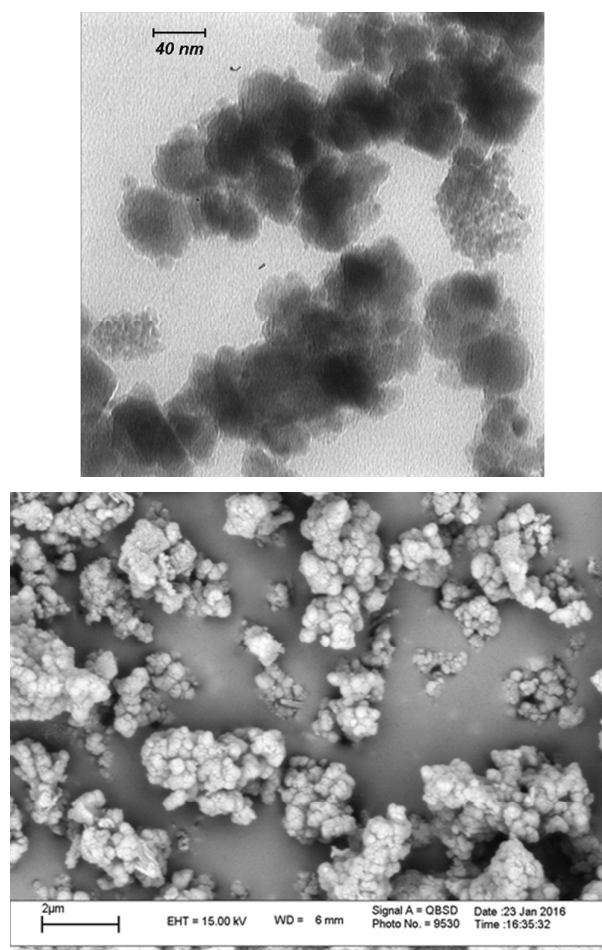


**Figure 8** TEM image of  $\text{Fe}_3\text{O}_4@\text{SiO}_2/\text{EP.EN.EG}@\text{Cu}$  after five times reuse (a), SEM image of  $\text{Fe}_3\text{O}_4@\text{SiO}_2/\text{EP.EN.EG}@\text{Cu}$  after five times reuse

The catalytic activity of  $\text{Fe}_3\text{O}_4@\text{SiO}_2/\text{EP.EN.EG}@\text{Cu}$  was compared with various reported catalysts in the literature<sup>46-50</sup> in the case of reduction of 4-nitrophenol. It was observed that  $\text{Fe}_3\text{O}_4@\text{SiO}_2/\text{EP.EN.EG}@\text{Cu}$  promotes the yield of products and reduces the reaction time effectively in comparison with other catalysts. So,  $\text{Fe}_3\text{O}_4@\text{SiO}_2/\text{EP.EN.EG}@\text{Cu}$  can be considered as efficient catalyst in reduction of nitro aryl compounds. (Table 5)

**Table 5** Comparison of various catalysts for reduction of 4-nitrophenol to 4-

Entry	Catalyst	Temp(°C)	Time(h)	Yield(%)	Ref.
1	$\text{CuBr}_2$	RT	3.5	88	46
2	Cu NPs	50	5	66	47
3	Ru(0)-supported on AT-Mont	Reflux	12	65	48
4	$\text{NiCo}_2\text{O}_4$	80	1.5	90	49
5	$\text{Ni/SiO}_2$	100	7	100	50
6	$\text{Fe}_3\text{O}_4@\text{SiO}_2/\text{EP.EN.EG}@\text{Cu}$	50	15 (min)	98	Present work

aminophenol

## Experimental

The melting point of the products was determined with an Electrothermal Type 9100 melting point apparatus. The FT-IR spectra were recorded on an Avatar 370 FT-IR

Thermal Nicolet spectrometer. Mass spectra were recorded on a 5973 Network Mass Selective Detector. The  $^1\text{H}$ NMR spectra were recorded on a Bruker AC 400 MHz instrument in  $\text{DMSO-d}_6$ . Thermogravimetric analysis (TGA) was performed on a Shimadzu Thermogravimetric Analyzer (TG-50). Transmission electron microscope (TEM) images were acquired on a TEM microscope Leo 912 AB120 KV Zeiss Germany. Elemental compositions were determined with a Leo 1450 VP scanning electron microscope equipped with an SC7620 energy dispersive spectrometer (SEM-EDS) presenting a 133 eV resolution at 20 KV. Inductively coupled plasma (ICP) was obtained using a Varian, VISTA-PRO, CCD, Australia. X-ray diffraction (XRD) patterns were collected using a Braker D4 X-Ray diffractometer with Ni-filtered Cu KR radiation (40KV, 30MA). The UV-Vis spectra were recorded on a Philips PUB 700 spectrophotometer with a quartz cuvette (path length = 1 cm) at 50 °C.

### **Synthesis of $\text{Fe}_3\text{O}_4@\text{SiO}_2$**

The synthesis of core-shell  $\text{Fe}_3\text{O}_4@\text{SiO}_2$  microspheres was carried out by a Stöber sol-gel method.<sup>29</sup> An aqueous dispersion of  $\text{Fe}_3\text{O}_4$  nanoparticles (6 ml,  $0.05 \text{ g ml}^{-1}$ ) were dissolved into a mixture of absolute ethanol (560 ml), deionized water (140 ml). Ammonia solution (28 wt%, 10 ml) was then added to the mixture under ultrasound for 20 min. Then, 8.0 ml tetraethyl ortosilicate (TEOS) was dropped into the mixture under stirring for 12 h. The acquired silica coated  $\text{Fe}_3\text{O}_4$  nanoparticles were separated by using a magnet, consequently washed with ethanol several times and dried under vacuum.

### **General procedure for the preparation $\text{Fe}_3\text{O}_4@\text{SiO}_2/\text{EP.EN.EP}$**

$\text{Fe}_3\text{O}_4@\text{SiO}_2$  (1 g) was added to the solution of epibromohydrin (1 ml) in ethanol (3 ml) and the mixture was stirred at 60°C. After 5h, the solvent was removed and the resulting solid was washed with ethanol and dried at 80°C. Then the dried precipitate was

suspended in ethylenediamine (5ml). The reaction mixture was stirred at 60 °C for 24h, after completion the product was separated by an external magnet, washed with MeOH and dried at 80 °C, the dried powder was mixed and stirred in epibromohydrin (1 ml) and ethanol (3 ml) at 60 °C for 5h, the resulting solid material was separated by an external magnet, washed with MeOH and dried at 80 °C.

**General procedure for the preparation of copper nanoparticles loaded on magnetic core ( $\text{Fe}_3\text{O}_4@\text{SiO}_2/\text{EP.EN.EG}@\text{Cu}$ )**

In first step,  $\text{Fe}_3\text{O}_4@\text{SiO}_2/\text{EP.EN.EP}$  (0.5 gr) was activated at room temperature for 1h in the presence of 5ml NaOH solution ( $0.1 \text{ mol L}^{-1}$ ), after separation, the activated catalyst ( $\text{Fe}_3\text{O}_4@\text{SiO}_2/\text{EP.EN.EG}$ ) washed with water and ethanol several times. In second step,  $\text{Cu}(\text{OAc})_2$  (0.25 gr) dissolved in absolute EtOH (5 ml) and stirred at room temperature for 4h with 0.5 gr activated catalyst. Then, solution of sodium borohydride (10.0 ml,  $0.15 \text{ mol L}^{-1}$ ) was added dropwise to the mixture and stirred under Ar atmosphere for 2 h. Finally, nanocatalyst collected by magnetic separation, washed with MeOH and dried under vacuum at room temperature for 8h.

**General procedure for reduction of nitro compounds in the presence of  $\text{Fe}_3\text{O}_4@\text{SiO}_2/\text{EP.EN.EG}@\text{Cu}$**

Suspension of  $\text{NaBH}_4$  (3 mmol) in  $\text{H}_2\text{O}$  (3 ml) was added to nitro compound (1 mmol), then stirred at 50 °C in presence of  $\text{Fe}_3\text{O}_4@\text{SiO}_2/\text{EP.EN.EG}@\text{Cu}$  (0.05gr) in water. The reaction progress was monitored by TLC, after the completion of the reaction the catalyst was taken out with external magnet and washed with ethanol. The reaction mixture was extracted with ethyl acetate and the combined organic layer was dried with

Na<sub>2</sub>SO<sub>4</sub>. The product was purified by column chromatography by using hexane-ethyl acetate as solvent system in different concentration to obtain the pure compound.

**p-Toluidine (Table 3, Entry 6):** FT-IR (KBr, cm<sup>-1</sup>): 3417, 3336, 3220, 3009, 2913, 2859, 1623, 1515, 1268, 1176, 813. <sup>1</sup>H NMR (400 MHz, DMSO-d<sub>6</sub>): 6.83 (d, *J* = 12 Hz, 2H, Ph), 6.49(d, *J* = 12 Hz, 2H, Ph), 4.78(s, 2H, NH<sub>2</sub>), 2.14 (s, 3H, Me). MS (EI): *m/z* (%) 107 [M<sup>+</sup>].

**N,N'-(4-amino-1,2-phenylene)diacetamide (Table 3, Entry 11):** FT-IR (KBr, cm<sup>-1</sup>): 3395, 3331, 3227, 3056, 1654, 1590, 1511, 1438, 1360, 1281. <sup>1</sup>H NMR (400 MHz, DMSO-d<sub>6</sub>): 9.22 (s, 2H, NH), 8.26-8.23 (m, 1H, Ph), 7.85 (dd, *J* = 12 Hz, *J* = 3.2 Hz, 1H, Ph), 6.74 (d, *J* = 12 Hz, 1H, Ph), 6.51 (s, 2H, NH<sub>2</sub>), 2.08 (s, 3H, Me).

**4-amin acetophenon (Table 3, Entry 12):** FT-IR (KBr, cm<sup>-1</sup>): 3395, 3331, 3227, 3056, 1654, 1590, 1511, 1438, 1360, 1281. <sup>1</sup>H NMR (400 MHz, DMSO-d<sub>6</sub>): 7.67 (d, *J* = 12 Hz, 2H, Ph), 6.56 (d, *J* = 12 Hz, 2H, Ph), 6.04 (s, 2H, NH<sub>2</sub>), 2.39 (s, 3H, Me). MS (EI): *m/z* (%) 135 [M<sup>+</sup>].

**4-Aminobenzoic acid (Table 3, Entry 13):** FT-IR (KBr, cm<sup>-1</sup>): 3460, 3381, 3363, 3235, 2978, 2823, 2671, 2594, 1665, 1624, 1600, 1572, 1442, 1421, 1312, 1291. <sup>1</sup>H NMR(400 MHz, DMSO-d<sub>6</sub>): 12.0(br, 1H, OH), 7.62(d, *J* = 12 Hz, 2H, Ph), 6.54(d, *J* = 8 Hz, 2H, Ph), 5.88(s, 2H, NH<sub>2</sub>). MS (EI): *m/z* (%) 137[M<sup>+</sup>].

## Conclusion

In summary, we report the preparation and characterization of novel designed Fe<sub>3</sub>O<sub>4</sub>@SiO<sub>2</sub>/EP.EN.EG@Cu catalyst. This catalyst demonstrate excellent catalytic performance in reduction of aromatic nitro compounds. The advantages of this catalytic

system are: (a) ease of preparation, use and separation of catalyst (b) the mild reaction conditions, (c) short reaction times and (d) high yields of substituted amines.

## Notes and references

<sup>a</sup>Department of Chemistry, Faculty of Sciences, Ferdowsi University of Mashhad, Mashhad, Iran.

<sup>b</sup>Department of Chemistry, Shiraz University of Technology, Shiraz, 71555-313, Shiraz, Iran.

\* Corresponding author: E-mail: heshghi@ferdowsi.um.ac.ir

1. S. V. Ley, A. W. Thomas, *Angew. Chem. Int. Ed.*, 2003, **42**, 5400.
2. S. Reymond, J. Cossy, *Chem. Rev.*, 2008, **108**, 5359.
3. N. Yan, C. Xiao, Y. Kou, *Coord. Chem. Rev.*, 2010, **254**, 1179.
4. A. Corma, H. García, A. Moussaif, M. J. Sabater, R. Zniber, A. Redouane, *Chem. Commun.*, 2002, 1058.
5. J. Sun, G. Yu, L. Liu, Z. Li, Q. Kan, Q. Huob, J. Guan, *Catal. Sci. Technol.*, 2014, **4**, 1246.
6. V. Polshettiwar, R. Luque, A. Fihri, H. Zhu, M. Bouhrara, J. M. Basset, *Chem. Rev.*, 2011, **111**, 3036.
7. Y. Yang, Z. H. Lu, Y. Hu, Z. Zhang, W. Shi, X. Chen, T. Wang, *RSC Adv.*, 2014, **4**, 13749.
8. D. Astruc, F. Lu, J. R. Aranzaes, *Angew. Chem. Int. Ed.*, 2005, **44**, 7852.
9. I. Nakamura, Y. Yamanoi, T. Yonezawa, T. Imaoka, K. Yamamoto, H. Nishihara, *Chem. Commun.*, 2008, 5716.
10. I. Nakamura, Y. Yamanoi, T. Imaoka, K. Yamamoto, H. Nishihara, *Angew. Chem. Int. Ed.*, 2011, **50**, 5830.
11. H. Yang, K. Nagai, T. Abe, H. Homma, T. Norimatsu, R. Ramaraj, *Appl. Mater. Interfaces.*, 2009, **1**, 1860.
12. (a) E. W. Wong, M. J. Bronikowski, M. E. Hoenk, R. S. Kowalczyk, B. D. Hunt, *Chem. Mater.*, 2005, **17**, 237; (b) M. Esmaeilpour, J. Javidi, F. Nowroozi Dodeji, H. Hassannezhad, *J. Iran. Chem. Soc.*, 2014, **11**, 1703.
13. Y. M. Huh, E. S. Lee, J. H. Lee, Y. W. Jun, P. H. Kim, C. O. Yun, J. H. Kim, J. S. Suh, *Adv. Mater.*, 2007, **19**, 3109.

14. C. Alexiou, R. Jurgons, R. Schmid, A. Hilpert, C. Bergemann, F. Parak, H. Iro, *J. Magn. Magn. Mater.*, 2005, **293**, 389; (b) J. L. Zhang, R. S. Srivastava, R. D. K. Misra, *Langmuir*, 2007, **23**, 6342.
15. M. F. Kircher, U. Mahmood, R. S. King, R. Weissleder, L. A. Josephson, *Cancer Res.*, 2003, **63**, 8122; (b) J. Jaber, E. Mohsen, *Colloids Surf. B.*, 2013, **102**, 265.
16. Y. Zhu, L. P. Stubbs, F. Ho, R. Liu, C. P. Ship, J. A. Maguire, N. S. Hosmane, *Chem Cat Chem.*, 2010, **2**, 365.
17. R. B. Nasir Baig, R. S. Varma, *Chem. Commun.*, 2012, **48**, 6220.
18. B. Dong, D. L. Miller, C. Y. Li, *J. Phys. Chem. Lett.*, 2012, **3**, 1346.
19. F. Zhang, J. Jin, X. Zhong, S. Li, J. Niu, R. Li, J. Ma, *Green Chem.*, 2011, **13**, 1238.
20. S. Luo, X. Zheng, J. P. Cheng, *Chem. Commun.*, 2008, **44**, 5719.
21. J. Zhang, Y. Wang, H. Ji, Y. We, N. We, N. Wu, B. Zuo, O. Wang, *J. Catal.*, 2005, **229**, 114.
22. Y. Sun, G. Liu, H. Gu, T. Huang, Y. Zhang, H. Li, *Chem. Commun.*, 2011, **47**, 2583.
23. Y. Jang, S. Kim, S. W. Jun, B. H. Kim, S. Hwang, I. K. Song, B. M. Kim, T. Hyeon, *Chem. Commun.*, 2011, **47**, 3601.
24. F. A. Khan, J. Dash, C. Sudheer, R. K. Gupta, *Tetrahedron Lett.*, 2003, **44**, 7783.
25. G. Rai, J. M. Jeong, Y. S. Lee, H. W. Kim, D. S. Lee, J. K. Chung, M. C. Leea, *Tetrahedron Lett.*, 2005, **46**, 3987.
26. Y. Shen, Y. Su, Y. Ma, *RSC Adv.*, 2015, **5**, 7597.
27. F. Figueras, B. Coq, *J. Mol. Catal. A: Chem.*, 2001, **173**, 223.
28. C. Lagrost, L. Preda, E. Volanschi, P. Hapiot, *J. Electroanal. Chem.*, 2005, **585**, 1.
29. R. M. Magdalene, E. G. Leelamani, G. N. M. Nanje, *J. Mol. Catal. A: Chem.*, 2004, **17**, 223.
30. F. Cardenas-Lizana, S. Gomez-Quero, M. A. Keane, *Catal. Commun.*, 2008, **9**, 475.
31. Z. Duan, G. Ma, W. Zhang, *Bull. Korean Chem. Soc.*, 2012, **33**, 4003.
32. N. Yan, Y. Yuan, P. J. Dyson, *Dalton Trans.*, 2013, **42**, 13294.
33. W. Li, Y. Deng, Z. Wu, X. Qian, J. Yang, Y. Wang, D. Gu, F. Zhang, B. Tu, D. Zhao, *J. Am. Chem. Soc.*, 2011, **133**, 1583.
34. F. Adam, K. M. Hello, H. Osman, *Chin. J. Chem.*, 2010, **28**, 2383.
35. N. Razavi, B. Akhlaghinia, *RSC Adv.*, 2015, **5**, 12372.
36. G. Bai, L. Shi, Z. Zhao, Y. Wang, M. Qiu, H. Dongm, *Mater Lett.*, 2013, **96**, 93.
37. S. Rezazadeh, B. Akhlaghinia, E. K. Goharshadi, H. Sarvari, *J. Chin. Chem. Soc.*, 2014, **61**, 1108.

38. A. K. Shil, D. Sharma, N. R. Guha, P. Das, *Tetrahedron Lett.*, 2012, **53**, 4858.
39. P. S. Kumar, K. M. L. Rai, *Chem. Pap.*, 2012, **66**, 772.
40. L. Sardari, J. L. Arora, S. Ferguson, S. Alfred, *Mol. Cryst. Liq. Cryst.*, 1970, **10**, 243.
41. J. B. Wright, C. M. Hall, H. G. Johnson, *J. Med. Chem.*, 1978, **21**, 930.
42. K. Anil Kumar, K. S. Shruthi, N. Naik, D. Channe Gowda, *E-J. Chem.*, 2008, **59**, 914.
43. Y. Tateoka, T. Kimura, K. Watanabe, I. Yamamoto, I. Kang Hob, *Chem. Pharm. Bull.*, 1987, **35**, 778.
44. Y. Motoyama, M. Taguchi, N. Desmirel, S. H. Yoon, I. Mochida, H. Nagashima, *Chem. Asian J.*, 2014, **9**, 71.
45. B. Raju, R. B. Ragul, N. Sivasankar, *Indian J. Chem.*, 2009, **48B**, 1315.
46. H. K. Kadam, S. G. Tilve, *RSC Adv.*, 2012, **2**, 6057.
47. Z. Duan, G. Ma, W. Zhang, *Bull. Korean Chem. Soc.*, 2012, **33**, 4003.
48. P. P. Sarmah, D. K. Dutta, *Green Chem.*, 2012, **14**, 1086.
49. N. S. Chaubal, M. R. Sawant, *J. Mol. Catal. A: Chem.*, 2007, **261**, 232.
50. Y. Zheng, K. Ma, H. Wang, X. Sun, J. Jiang, C. Wang, R. Li, J. Ma, *Catal. Lett.*, 2008, **124**, 268.

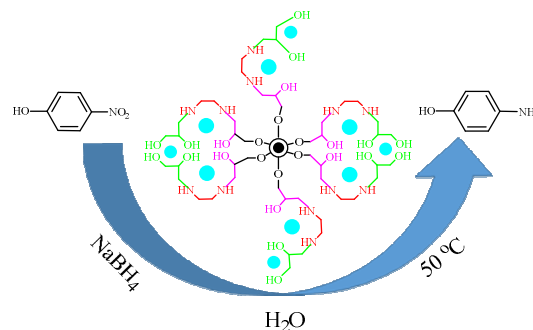


**Generation of Cu nanoparticles on novel designed  $\text{Fe}_3\text{O}_4@\text{SiO}_2/\text{EP.EN.EG}$  as reusable nanocatalyst for the reduction of nitro compounds**

Maryam Rajabzadeh<sup>a</sup>, Hossein Eshghi<sup>a\*</sup>,  
Reza Khalifeh<sup>b</sup>, Mehdi Bakavoli<sup>a</sup>,

1. Reusable magnetic Cu nanocatalyst was designed and characterized

2. An efficient and mild method for the reduction of aromatic nitro compounds



**Graphical Abstract**